BEC preprints 2026.5
https://doi.org/10.26124/becprep.2026-0005

Conceptual Communication

Cite
Gnaiger E (2026) Mapping the scope of metabolic flexibility by respiratory flux control: Bioenergetic cluster analysis of mitochondrial fitness. BEC preprints 2026.5. https://doi.org/10.26124/becprep.2026-0005

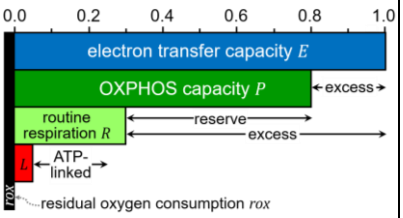

Received 2026-09-24
Online 2026-09-24

Conflict of interests
EG is founder and CEO of Oroboros Instruments.

Keywords
bioenergetic cluster analysis
bioenergetic fitness index
coupling efficiency
electron transfer
excess capacity
leak respiration
oxidative capacity
oxidative phosphorylation
routine respiration
routine-ATP coupling ratio
routine-ATP control efficiency

Mapping the scope of metabolic flexibility by respiratory flux control: Bioenergetic cluster analysis of mitochondrial fitness

Erich Gnaiger

Oroboros Instruments, Innsbruck, Austria
Corresponding author: erich.gnaiger@oroboros.at

Summary

Cell respiration studied in coupling-control states of living cells provides diagnostic information on cellular bioenergetics and mitochondrial function. Routine respiration R is under *cell physiological* control of aerobic ATP demand within limits set by mitochondrial performance. By contrast, *mitochondrial* coupling control is assessed by relating leak respiration L – when aerobic ATP turnover is arrested – to electron transfer capacity E when oxidative phosphorylation is decoupled from electron transfer. E is not a surrogate for the capacity of oxidative phosphorylation (OXPHOS, P) which requires OXPHOS analysis with permeabilized cells.

Normalization of O_2 consumption by cell count and cell size provides information on cell-specific respiration, whereas normalization to a mitochondrial marker expresses respiration independent of cell-metric variables. Cell respiration normalized to E or R, determined within the coupling-control protocol, yields the respiratory flux control indices:

- coupling efficiency, $j_{E-L} = (E-L)/E$
- $E-R$ excess ratio, $j_{E-R} = (E-R)/E$
- R-ATP coupling ratio, $j_{RLE} = (R-L)/E$
- R-ATP control efficiency, $j_{R-L} = (R-L)/R$

Bioenergetic cluster analysis (BCA) provides fundamental quality control by identifying apparent artifacts. More importantly, BCA reveals mechanistic relationships among flux control indices for improved evaluation of mitochondrial fitness. Trajectories and breakpoints in BCA define the theoretical scope of metabolic flexibility. The direction of a respiratory change alone does not necessarily distinguish

physiological adaption from emerging dysfunction. Precision OXPHOS analysis delivers the next level.

Introduction: Three respiratory coupling states are addressed in the basic coupling-control protocol (CCP) applied to living cells with the corresponding mitochondrial (mt) rates of oxygen (O_2) consumption: (*1*) **Routine respiration** R is under cell physiological control of aerobic ATP turnover. (*2*) **Leak respiration** L compensates for proton leak, cation cycling, and proton slip in a mitochondrial resting state obtained after inhibition of aerobic ATP production. (*3*) Oxidative capacity or **electron transfer capacity** E is the maximum respiration obtained upon titrations of a protonophore (uncoupler) which dissipates the protonmotive force [1-4]. These respiratory rates are baseline-corrected for residual oxygen consumption rox quantified after inhibition of the mitochondrial electron transfer system ETS. Despite the widespread application of the CCP, which is also referred to as 'mitochondrial stress test' [5], interpretation frequently remains descriptive, and fundamental relationships among respiratory control indices are rarely exploited for quality control and mechanistic analysis [6]. A literature survey [5] demonstrates the need for a general quality-control and interpretative framework provided by bioenergetic cluster analysis [3,7].

Respiratory rates (capacities) are expressed as O_2 flow per cell [amol·s^{-1}·x^{-1}] when normalization is achieved by cell count (number of cells [x]) or O_2 flux per cell size [pmol·s^{-1}·mg^{-1}], expressing cell size as protein or wet mass [8]. Alternatively, O_2 flux is normalized to citrate synthase activity as a mt-matrix marker [8]. Changes of mt-marker enzymes and mt-size reveal complex adaptive plasticity [9,10,11]. Variability of results depends not only on the respirometric method [3,12] but on the measurement of the normalization parameter. In contrast, flux control ratios are obtained by internal normalization as dimensionless ratios of oxygen consumption in different coupling states of mitochondrial respiration. Therefore, these ratios provide diagnostic information on mitochondrial function independent of cell count and mitochondrial density in the cells.

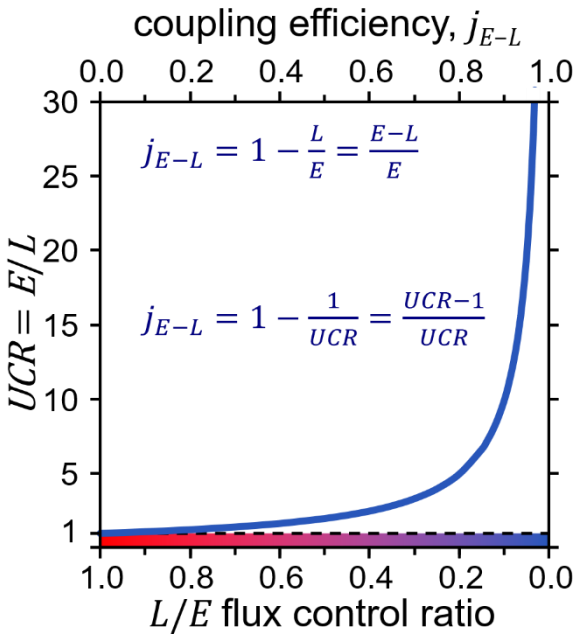

Figure 1. Uncoupling-control ratio UCR – ranging from 1 to infinity – related non-linearly to the L/E flux control ratio and coupling efficiency j_{E-L} ranging from 0 to 1.

The concept of respiratory control ratios has a long tradition in bioenergetics to analyze respiratory parameters independent of mitochondrial content. In isolated mitochondria (mt) and other mt-

preparations, the ratio of oxidative phosphorylation (OXPHOS) capacity P to leak respiration L is the respiratory acceptor control ratio ($RCR = P/L$) [6,13]. Likewise, the ratio of oxidative capacity E to L is the uncoupling-control ratio ($UCR = E/L$). The theoretical range of the RCR and UCR spans from 1 (zero coupling) to infinity (fully coupled). This causes a statistical problem of nonlinearity and asymmetric standard deviations of the RCR and UCR. Therefore, the 'classical' RCR and UCR are replaced by the L/P and L/E coupling-control ratios and corresponding control efficiencies which are bounded between 0 and 1 (**Figure 1**).

A major limitation of the CCP with living cells is the lack of a method to induce maximum biochemical work performance as the ultimate physiological determinant of bioenergetic fitness [6]. Biochemical work requires respiration coupled to phosphorylation of ADP. Hence, the maximum aerobic OXPHOS capacity underlying biochemical work in living cells – comparable to the maximum oxygen consumption rate (V_{O2max}) measured by spiroergometry – can be determined only as OXPHOS capacity P in permeabilized cells [14]. The analogy between (maximal) E and ergometric V_{O2max} [5] is therefore misleading. ADP and inorganic phosphate are not freely permeable across the intact plasma membrane. Determination of P requires mitochondrial preparations allowing control of saturating ADP and phosphate concentrations. Depending on mitochondrial type, OXPHOS capacity P may be limited by the phosphorylation system and thus be lower than ET capacity E [6,14,15]. The corresponding $E–P$ excess ratio, $(E–P)/E$, can be extrapolated from permeabilized to living cells, allowing the important distinction between $E–R$ excess capacity and the actual spare or reserve capacity, $P–R$.

Notably, routine respiration can be assessed only in living cells, since physiological control of aerobic ATP turnover is disrupted in mitochondrial preparations. The ambiguous term 'basal respiration' [2] is frequently used instead of routine respiration; for harmonization of terminology, see [3]. Basal respiration may be understood as minimum leak respiration in mitochondrial preparations and living cells, whereas routine respiration retains physiological ATP demand. At the organism level, basal metabolic rate (BMR) is the minimum rate of energy expenditure compatible with life under standardized conditions [16]. Routine respiration sustains cellular activities influenced by substrate availability and variable growth conditions during the cell cycle. Thus, 'basal' and 'routine' represent distinct experimental concepts.

Bioenergetic cluster analysis (BCA) is introduced as a conceptual and quantitative framework for integrating respiratory flux control ratios and flux control indices. BCA visualizes fundamental constraints on flux-control relationships and defines trajectories, breakpoints, and the theoretical scope of metabolic flexibility. This framework extends interpretation beyond whether an individual respiratory variable increases or decreases, toward evaluating physiological adaption and evolutionary adaptation, emerging mitochondrial dysfunction, and mitochondrial fitness.

1. Respiratory flux control ratios and reference flux ratios

Respiratory flux control ratios are respiratory rates Y in a defined respiratory state normalized for the rate Z in a respiratory reference state (**Box 1**). This eliminates the variability of independently measured normalization parameters [8]. **Flux control ratios** FCR are calculated from rates in sequential respiratory states within a substrate-uncoupler-inhibitor titration (SUIT) protocol (**Figure 2a**).

When comparing experimental groups, respiratory rates of different samples can be expressed by normalization to rate $Z°$ of the reference group. The flux control ratio of the reference group is $FCR° \stackrel{\text{def}}{=} j° = Y°/Z°$. The corresponding **reference flux ratios** j are $e = E/E°$, $r = R/E°$, $l = L/E°$, and $p = P/E°$ (**Box 2**). Reference flux ratios j (normalized for $Z°$) are different from flux control ratios FCR (normalized for Z). Exclusively $j°$ of the reference group is a proper FCR (**Figure 2b**). Reference flux ratios require external normalization for relating respiratory rates between assays with different experimental groups, instead of merely comparing $FCRs$ between experimental groups (**Figure 2a**).

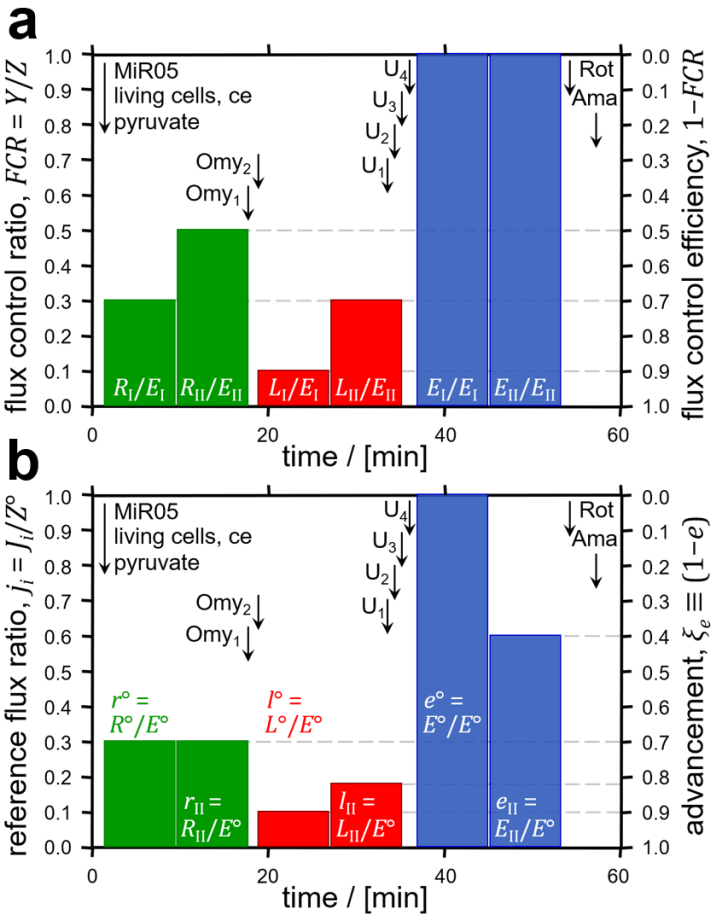

Figure 2. Flux control ratios and reference flux ratios of two cohorts, I and II, in the coupling-control protocol. MiR05 is mitochondrial respiration medium. Titrations are indicated for oligomycin (Omy), uncoupler (U, CCCP), and finally rotenone and antimycin A (Rot, Ama) to measure residual oxygen consumption for baseline correction. **(a)** Flux control ratios FCR and flux control efficiencies calculated for each cohort independently with the reference flux $Z = E_{\mathrm{I}}$ or $Z = E_{\mathrm{II}}$ in cohort I and II, respectively. The different L/E ratios indicate a qualitative change of mitochondrial function. **(b)** Cohort II defined as reference ($Z° = E° \stackrel{\text{def}}{=} E_{\mathrm{I}}$). The relative ET capacity of cohort II is $e_{\mathrm{II}} = 0.6$, indicating an extent (advancement) of relative change of 0.4. The values $r°$ and r_{II} are 0.3, but routine-ATP coupling (net) ratios, $j°_{RLE} = r°-l°$ and $j_{\mathrm{II}RLE} = r_{\mathrm{II}}-l_{\mathrm{II}}$, differ. The overall changes result from the combined mechanisms of coupling-control efficiency (a) and ET capacity (b).

2. Respiratory flux control efficiencies

SUIT protocols are designed to quantify instantaneous step changes of respiratory rates in response to metabolic control variables, such as oligomycin (decrease from R to L) or uncoupler (increase from L to E). Corresponding flux control efficiencies are calculated from sequential respiratory states within a SUIT protocol and express the step changes (Δ) relative to the higher value that is taken as the reference Z.

2.1. Coupling efficiency, j_{E-L}

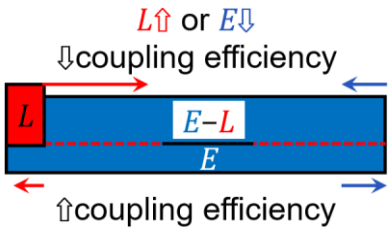

The coupling efficiency, $j_{E-L} = (E-L)/E$, is the relative scope from leak respiration to oxidative capacity. At minimum efficiency of zero, only leak respiration remains without ATP formation in OXPHOS ($L = E$). At maximum coupling efficiency of 1, leak respiration is zero ($L = 0$). A decrease of j_{E-L} is due to either an increase of L ($L⇧$) at constant $E = E°$ or a decrease of E ($E⇩$) at constant $L = L°$ to the breakpoint when E declines to the value of $L°$. In the present context, it is convenient to use the short term **coupling efficiency**. More specifically, this quantity is referred to as the 'oxidative coupling-control efficiency', to distinguish $(E-L)/E$ from the OXPHOS coupling efficiency, $j_{PLE} = (P-L)/E$, determined in mt-preparations (**Box 1**). In contrast, thermodynamic (ergodynamic) efficiency is strictly defined as the product of output/input flux ratios and force ratios [6]. E can be considered as the input oxidative capacity. Correspondingly, $E-L$ is the potential output flux of net respiration available for ATP production.

2.2. $E-R$ excess ratio, j_{E-R}

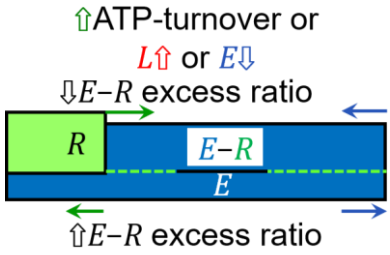

The $E-R$ excess ratio, $j_{E-R} = (E-R)/E$, is the scope by which routine respiration can be increased relative to oxidative capacity, if the phosphorylation system does not exert a limiting effect on R. At limiting capacity of the phosphorylation system ($E>P$), the *excess* capacity ($E-R$) overestimates the ATP-coupled *reserve* capacity ($P-R$). The R/E ratio and $E-R$ excess ratio are influenced by physiological state (e.g. kinetic control by ADP and inorganic phosphate concentrations), coupling, OXPHOS capacity, and oxidative capacity. Generally, flux control efficiencies must not be interpreted as efficiency in the thermodynamic sense. Flux control 'efficiency' in relation to the ***E−R* excess ratio** refers to the concept of flux control (**Eq. 1**). $E-R$ is not an output flux but represents the respiratory excess capacity. The term 'reserve capacity' – frequently used for the difference $E-R$ – conceals the fundamental bioenergetic distinction between E and P – oxidative capacity versus OXPHOS capacity [15].

2.3. Routine-ATP coupling ratio, j_{RLE}

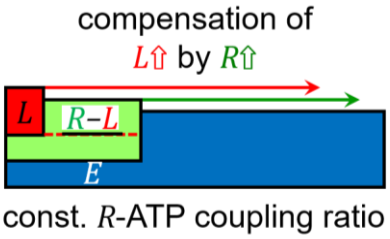

The R-ATP coupling ratio, $j_{RLE} = (R-L)/E$, represents the fraction of E that supports ATP production during routine respiration. If an increase in L is compensated by an equivalent increase in R at constant E, ATP turnover remains constant up to the breakpoint when R cannot be increased beyond the limiting OXPHOS capacity P. Up to the breakpoint, the physiologically relevant ***R*-ATP coupling ratio** is maintained constant even though coupling efficiency declines. Considering depression of routine activity, $(R-L)/E$ is the relative scope by which routine respiration can be reduced in metabolic shutdown beyond the shifts in mitochondrial properties [17].

2.4. Routine-ATP control efficiency, j_{R-L}

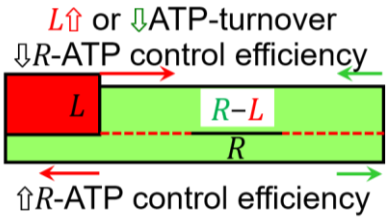

The R-ATP control efficiency, $j_{R-L} = (R-L)/R$, is the routine respiration used for ATP generation normalized for R. When $j_{R-L} = 0$, there is no ATP generation in routine respiration and only leak respiration remains ($L = R$). At maximum R-ATP control efficiency of 1, leak respiration is zero ($L = 0$). The ***R*-ATP control efficiency** j_{R-L}, uses $Z = R$ as the reference rate, in contrast to the common reference rate $Z = E$ shared by j_{E-L}, j_{E-R}, and j_{RLE}. The terms j_{R-L} and j_{RLE} contain the ATP-coupled respiratory rate or net routine rate, $R-L$, which must not be confused with the direct measurement of ATP production.

2.5. Two formats and two independent flux control efficiencies

Respiratory flux control efficiencies are expressed in two equivalent formats [6]. (*1*) The difference of oxidative capacity E and leak respiration L is the scope of respiration from the minimum resting rate to the maximum decoupled rate ($E-L$). The scope is divided by E (reference rate Z) to obtain the coupling efficiency ranging from 0 to 1, $(E-L)/E$. (*2*) This expression contains the L/E ratio (Y/Z; **Box 1**) – the coupling efficiency is $E/E - L/E$ (**Eq. 1a**),

$$j_{Z-Y} = \frac{Z-Y}{Z} = 1 - \frac{Y}{Z} \qquad j_{E-L} = \frac{E-L}{E} = 1 - \frac{L}{E} \qquad \text{(Eq. 1a)}$$

$$j_{Y_1Y_2Z} = \frac{Y_1-Y_2}{Z} = \frac{Y_1}{Z} - \frac{Y_2}{Z} \qquad j_{RLE} = \frac{R-L}{E} = \frac{R}{E} - \frac{L}{E} \qquad \text{(Eq. 1b)}$$

Two flux control efficiencies, $j_{E-L} = 1-L/E$ and $j_{E-R} = 1-R/E$ are calculated directly from the fundamental L/E and R/E flux control ratios (**Eq. 1a**). The two additional flux control efficiencies, j_{RLE} (**Eq. 1b**) and j_{R-L}, are derived from these $FCRs$. The R-ATP coupling ratio is the difference between the fundamental $FCRs$, $j_{RLE} = R/E-L/E$. The R-ATP control efficiency is calculated from their ratio, $j_{R-L} = 1 - \frac{L/E}{R/E} = 1 - \frac{L}{R}$ (**Box 2**).

Box 1. Flux control efficiencies derived from the coupling-control protocol[#] defined in the formats of flux control ratios FCR and scope of respiratory capacity.

FCR	Flux control efficiency	Symbol	FCR format	Scope format
L/E	coupling efficiency	j_{E-L}	$1-L/E$	$(E-L)/E$
R/E	$E-R$ excess ratio	j_{E-R}	$1-R/E$	$(E-R)/E$
	routine-ATP coupling ratio	j_{RLE}	$R/E-L/E$	$(R-L)/E$
L/R	routine-ATP control efficiency	j_{R-L}	$1-L/R$	$(R-L)/R$
	[#] OXPHOS coupling efficiency	j_{PLE}	$P/E-L/E$	$(P-L)/E$
	[#] OXPHOS reserve ratio	j_{PRE}	$P/E-R/E$	$(P-R)/E$
[#] P/E	[#] $E-P$ excess ratio	j_{E-P}	$1-P/E$	$(E-P)/E$
[#] L/P	[#] $P-L$ control efficiency	j_{P-L}	$1-L/P$	$(P-L)/P$

[#] P is measured in a respirometric OXPHOS protocol with permeabilized cells [6].

Box 2. Four respiratory control indices derived from two independent flux control ratios FCR, the L/E coupling-control ratio(1) and the R/E control ratio(2). Initial values in a respiratory standard model ($s°_{I}$) are set as $l° = L°/E° = 0.10$, $r° = R°/E° = 0.30$, and $p° = P°/E° = 0.80$. In model II ($s°_{II}$), $l°$, $r°$, and $p°$ increase together, maintaining r–l constant(3,4). Compare flux control ratios FCR (L/E and R/E), reference flux ratios ($l = L/E°$ and $r = R/E°$), and initial flux control ratios ($l° = L°/E°$ and $r° = R°/E°$).

FCR	$s°_{I}$	$s°_{II}$	Control index	Definition	Initial	$s°_{I}$	$s°_{II}$
$\frac{L}{E}$	0.10	0.30	coupling efficiency	$j_{E-L} = \frac{E-L}{E}$	$\frac{e°-l°}{e°}$	0.90	0.70
$\frac{R}{E}$	0.30	0.50	$E-R$ excess ratio	$j_{E-R} = \frac{E-R}{E}$	$\frac{e°-r°}{e°}$	0.70	0.50
$\frac{R}{E}-\frac{L}{E}$			R-ATP coupling ratio	$j_{RLE} = \frac{R-L}{E}$	$\frac{r°-l°}{e°}$	0.20	0.20
$\frac{L}{R}$	0.33	0.60	R-ATP control efficiency	$j_{R-L} = \frac{R-L}{R}$	$\frac{r°-l°}{r°}$	0.67	0.40
$\frac{P}{E}-\frac{L}{E}$			OXPHOS coupling efficiency	$j_{PLE} = \frac{P-L}{E}$	$\frac{p°-l°}{e°}$	0.70	0.70
$\frac{P}{E}-\frac{R}{E}$			OXPHOS reserve ratio	$j_{PRE} = \frac{P-R}{E}$	$\frac{p°-r°}{e°}$	0.50	0.50
$\frac{P}{E}$	0.80	1.00	$E-P$ excess ratio	$j_{E-P} = \frac{E-P}{E}$	$\frac{e°-p°}{e°}$	0.20	0.00
$\frac{L}{P}$	0.13	0.30	$P-L$ control efficiency	$j_{P-L} = \frac{P-L}{P}$	$\frac{p°-l°}{p°}$	0.88	0.70

(1) $\frac{L}{E} = \frac{R}{E} \cdot \frac{L}{R}$

(2) $\frac{R}{E} = \frac{L}{E} \cdot \frac{1}{L/R} = \frac{j_{RLE}}{j_{R-L}}$

(3) $j_{RLE} = j_{E-L} - j_{E-R}$

(4) $j_{R-L} = \frac{j_{RLE}}{1-j_{E-R}} = \frac{j_{RLE}}{r}$

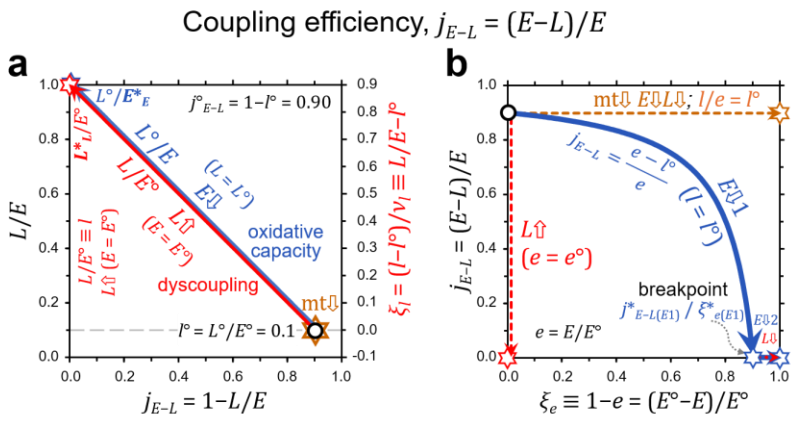

Figure 3. Coupling efficiency and respiratory control models. Circles: initial or control group (l° = 0.1; j°_{E-L} = 0.90). Asterisks: breakpoints or endpoints. Coupling model L⇧: increasing L at constant E = E°. Capacity model E⇩: decreasing E at constant L = L°. mt-Density model mt⇩: declining mt-density per cell at constant L/E, indicating preserved function per mt-marker. **(a)** L/E flux control ratio, coupling efficiency, and advancement of increasing L⇧, ξ_l (ν_l = 1; breakpoint $\boldsymbol{L^*_L} = e^\circ$) in contrast to decreasing E⇩ (breakpoint $\boldsymbol{E^*_E} = l^\circ$). No change at declining mt⇩ (initial and breakpoints are equal). **(b)** Decrease of coupling efficiency j_{E-L} with advancement ξ_e of decreasing ET capacity, $e = E/E^\circ$; $\nu_e = -1$ (Eq. 2). In a first phase E⇩1, E declines at constant $l = l^\circ$ to the breakpoint $j^*_{E-L(E1)}$ ($\boldsymbol{e^*_{E1}} = l^\circ$) and advancement $\xi^*_{e(E1)} = j^\circ_{E-L}$ (blue asterisk). $j^*_{E-L(E1)} = 0.0$ at $\xi^*_{e(E1)} = 1-l^\circ$ and $j_{E-L} = 0.5$ at $\xi_e = 1-2\cdot l^\circ$. When E decreases beyond breakpoint 1, leak declines (L⇩) with E⇩2 (capacity model). Dashed vertical arrow: increase of L at constant $e = e^\circ$ (coupling model L⇧). Dashed horizontal arrow: decrease of E and L (per cell) at decline of mitochondrial density and constant E and L per mt-marker (mt-density model mt⇩).

Box 3. Respiratory reference flux ratios j related to the advancement ξ_j with respect to the initial reference rate $Z^\circ = E^\circ$. ν_j is the stoichiometric number; $\nu_j = 1$ if $j>j^\circ$ (j⇧) and $\nu_j = -1$ if $j<j^\circ$ (j⇩). The reference or initial flux control ratio is FCR° ($e^\circ \stackrel{\text{def}}{=} 1$).

Name	Definition j_i, ξ_j		FCR°	
oxidative reference flux ratio	e	$= E/E^\circ$	e°	$= E^\circ/E^\circ = 1$
advancement of e	ξ_e	$= (e-e^\circ)/\nu_e \equiv e^\circ-e$ (E⇩)		
leak reference flux ratio	l	$= L/E^\circ$	l°	$= L^\circ/E^\circ$
advancement of l	ξ_l	$= (l-l^\circ)/\nu_l \equiv l-l^\circ$ (L⇧)		
routine reference flux ratio	r	$= R/E^\circ$	r°	$= R^\circ/E^\circ$
advancement of r	ξ_r	$= (r-r^\circ)/\nu_r \equiv r-r^\circ$ (R⇧)		
#OXPHOS reference flux ratio	p	$= P/E^\circ$	p°	$= P^\circ/E^\circ$
#advancement of p	ξ_p	$= (p-p^\circ)/\nu_p \equiv p-p^\circ$ (P⇧)		

Requires a separate SUIT protocol with permeabilized cells and saturating [ADP].

Mathematically, converting the two independent respiratory control efficiencies into two additional dependent quantities does not generate new information (**Box 2**). Instead, these expressions provide complementary views, mapping the same bioenergetic landscape from different angles by bioenergetic cluster analysis.

3. Advancement

The extent of change of respiratory rates between samples of cells can be expressed as the difference between rate j_i and the reference rate $j°$. The **advancement** ξ_j (**Eq. 2**),

$$\xi_j = \frac{j_i - j°}{\nu_j} \qquad \xi_e = \frac{e_i - e°}{\nu_e} \qquad \text{(Eq. 2)}$$

describes the extent of change of rates (j_i–$j°$) in a defined respiratory state of different experimental groups i. The stoichiometric numbers are $\nu_j = 1$ and $\nu_j = -1$ for increased ($j_i > j°$) and decreased ($j_i < j°$) controlling rates, respectively. $j°$ are rates in initial states at time $t°$ and different time points t (j_t) investigated in longitudinal experimental regimes. Alternatively, $j°$ is determined in a reference group (e.g. placebo control), whereas j_i describe experimental cohorts i (e.g. exercise or nutritional interventions; drug treatments), patient groups, or different populations and species in comparative physiology. Possibly $j°$ is defined as the average of a group for expressing the deviations of each individual data point from the average of the group. Discrete data of advancement are shown as continuous trajectories in a graphical representation of a numerical analysis of respiratory control models (**Figure 3**).

Flux control ratios are linked to flux control efficiencies (**Figure 2a**; **Box 1**). In turn, reference flux ratios are related to the advancement (**Figure 2b**; **Box 3**). Unlike flux control ratios, reference flux ratios are not limited to maximum values of one, if $e > e°$.

Translation of graphical representations into mathematical equations requires formal definitions of terms and symbols (**Box 3**). The concept of advancement is rooted in physical chemistry [18]. The extent (advancement) of chemical reactions is linked to changes of substrates or products i and their respective stoichiometric numbers ν_i [19]. Inserting $\nu_e = -1$ for diminishing e in the capacity model, Eq. 2 yields $\xi_e \equiv 1 - e$, since $e° \stackrel{\text{def}}{=} 1$. The decline of coupling efficiency with progressive loss of ET capacity follows a hyperbolic function, $j_{E-L} = (e - l°)/e$ (**Figure 3b**).

4. Bioenergetic cluster analysis

When results are expressed as ratios of respiratory rates Y/Z, it is tempting to interpret a change of the ratio to be caused by a change of the background rate Y, assuming the value Z to be constant. However, Z of the experimental cohort may change relative to $Z°$ of the control group of cells (**Figure 2**). This control group may be represented by the initial time point in a longitudinal study, the placebo control, or the healthy reference group. The following analyses of respiratory flux control ratios and control efficiencies use models of respiratory flux control and bioenergetic cluster analysis (BCA), showing distinct regression lines to disentangle the contrasting effects on L/E (**Figure 3**) of changes (Δ) in the background rate $\Delta L/E°$ versus reference rate $\Delta E/E°$ (**Figure 4**).

4.1. Models of respiratory flux control

Differential models of respiratory control distinguish between the rate which controls changes of respiration – the mechanistic driver – and the controlled rates which are maintained constant up to a breakpoint (**Table 1**). The extent of change in the controlling rate, j–j°, is the advancement ξ_j as a measure of bioenergetic flexibility. The controlling rate j is the leak rate l in the coupling model, the routine rate r in the routine model, the oxidative rate e in the capacity model, and the combined decline of e, l, and p in the mitochondrial density model. The extent of change in the controlling rate may represent either a defect or a physiological *adaption*, distinguished from evolutionary *adaptation* across generations [20].

Table 1. Controlling rates defining the advancement ξ_j (Eq. 2) versus controlled rates maintained constant at increasing ξ_j up to breakpoints (l^*; r^*; e^*) defined by limiting conditions $L \le R \le P \le E$. Breakpoints of the controlling rates and stoichiometrically advancing rates (r as a function of l) are emphasized in bold font.

Model	Controlling rate	Constant rates	Limiting conditions	Breakpoint *1	Breakpoint *2	Figure
coupling	$L\Uparrow$	$(r-l)^\circ$, E°;	$L \le R \le E$	$\boldsymbol{l^*_{L1} = j^\circ_{E-R} + l^\circ}$	$\boldsymbol{l^*_{L2} = e^\circ \overset{\text{def}}{=} 1}$	4a
	$R\Uparrow$	j°_{RLE}		$\boldsymbol{r^*_{L1} = e^\circ}$	$r^*_{L2} = e^\circ$	
				$e^*_{L1} = e^\circ$	$e^*_{L2} = e^\circ$	
				$\xi^*_{l(L1)} = j^\circ_{E-R}$	$\xi^*_{l(L2)} = j^\circ_{E-L}$	
routine	$R\Uparrow$	e°, l°;	$R \le P \le E$	$\boldsymbol{r^*_{R\Uparrow} = p^\circ}$		4b
		j°_{E-L}		$e^*_{R\Uparrow} = e^\circ$		
				$l^*_{R\Uparrow} = l^\circ$		
				$\xi^*_{r(R\Uparrow)} = j^\circ_{PRE}$		
	$R\Downarrow$	e°, l°;	$R \ge L$	$\boldsymbol{r^*_{R\Downarrow} = l^\circ}$		
		j°_{E-L}		$e^*_{R\Downarrow} = e^\circ$		
				$l^*_{R\Downarrow} = l^\circ$		
				$\xi^*_{r(R\Downarrow)} = j^\circ_{RLE}$		
capacity	$E\Downarrow$	r°, l°, $(r-l)^\circ$;	$E \ge R \ge L$	$\boldsymbol{e^*_{E1} = r^\circ}$	$\boldsymbol{e^*_{E2} = l^\circ}$	4c
		j°_{R-L}		$r^*_{E1} = r^\circ$	$r^*_{E2} = l^\circ$	
				$l^*_{E1} = l^\circ$	$l^*_{E2} = l^\circ$	
				$\xi^*_{e(E1)} = j^\circ_{E-R}$	$\xi^*_{e(E2)} = j^\circ_{E-L}$	
mt-density	mt$\Downarrow$	$(r-l)^\circ$;	$E \ge R$	$\boldsymbol{e^*_{mt1} = \frac{j^\circ_{RLE}}{j^\circ_{PLE}}}$	$\boldsymbol{e^*_{mt2} = 1-e^\circ = 0}$	4d
	$E\Downarrow L\Downarrow R\Downarrow$	j°_{E-L}		$\boldsymbol{r^*_{mt1} = p^\circ \cdot \frac{j^\circ_{RLE}}{j^\circ_{PLE}}}$	$r^*_{mt2} = p^\circ \cdot (1-e^\circ)$	
				$\boldsymbol{l^*_{mt1} = l^\circ \cdot \frac{j^\circ_{RLE}}{j^\circ_{PLE}}}$	$\boldsymbol{l^*_{mt2} = l^\circ \cdot (1-e^\circ)}$	
				$\xi^*_{e(mt1)} = \frac{j^\circ_{PRE}}{j^\circ_{PLE}}$	$\xi^*_{e(mt2)} = e^\circ = 1$	

In a numerical analysis, the controlling rate is changed stepwise from an initial respiratory state at zero advancement to the breakpoint. Graphical representations highlight the breakpoints at which a further change of the controlling rate is not possible without adjustment of one or more controlled rates (**Figure 4**). The maximum possible advancement of a respiratory control pattern denotes how far the controlling rate can be changed experimentally up to a breakpoint, thus expressing the boundaries of metabolic flexibility. Further advancement beyond a breakpoint is limited by fundamental relationships between bioenergetic parameters (**Table 1**).

The coupling-control protocol with living cells involves sequential measurement of R, L, and E (**Figure 2**). A representative model uses the following flux control ratios in the initial state: $l° = L°/E° = 0.10$, $r° = R°/E° = 0.30$ (**Box 2;** $s°_{\mathrm{I}}$). A separate respirometric protocol is required with permeabilized cells to determine the OXPHOS capacity P at saturating ADP concentration and substrate combinations that support physiological OXPHOS capacity [14]. For example, $p° = P°/E° = 0.80$ (**Figure 4a1**).

a) Coupling model (**Figure 4a**): Dyscoupling is caused by increased leak respiration $L⇧$ (Δl at constant $e = e°$). This induces an equivalent increase of routine respiration ($L⇧1\ R⇧$; $\Delta r = \Delta l$). The compensatory increase in R maintains ATP turnover and thus $r–l$ constant at diminishing oxidative excess up to the breakpoint $\boldsymbol{r*_{L1}} = e°$. The corresponding breakpoint of leak respiration is $\boldsymbol{l*_{L1}} = 1–r°+l°$ at an advancement $\xi*_{l(L1)} = j°_{E–R}$. Then l advances maximally further (at constant $r = e°$) to $\boldsymbol{l*_{L2}} = e°$ at the breakpoint $\xi*_{l(L2)} = j°_{E–L}$ (**Table 1**). This increase in $L⇧2$ cannot be compensated by increasing R, but j_{RLE} declines proportionally with coupling efficiency. OXPHOS capacity increases in parallel with leak respiration to the point $P = E$ (**Figure 4a1**), as shown in ischemia-reperfusion injury of human cardiac mitochondria with high $E–P$ excess capacity [21]. Senescence-associated changes are analyzed in **Section 4.3**.

b) Routine model (**Figure 4b**): Routine respiration is stimulated or declines ($R⇧$ or $R⇩$; at constant mitochondrial properties) controlled by cellular aerobic ATP demand. The breakpoint for $R⇧$ at increasing aerobic ATP turnover is $\boldsymbol{r*_{R⇧}} = p°$ and is, therefore, limited by OXPHOS (reserve) capacity rather than ET (excess) capacity. The $E–R$ excess ratio, $(E–R)/E$, determines this breakpoint only if the excess oxidative capacity is zero at $P = E$ ($p° = e°$; **Figure 4b2**). The breakpoint in $R⇩$ is $\boldsymbol{r*_{R⇩}} = l°$. The boundaries of the routine model are set by the mitochondrial parameters, but the mechanisms of respiratory control are non-mitochondrial, activation or shut-down of aerobic cellular activity.

c) Capacity model (**Figure 4c**): When coupling efficiency is compromised by declining oxidative capacity at constant $L°$, it is theoretically possible that $E⇩1$ is without effect on R until the breakpoint at $\boldsymbol{e*_{E1}} = r°$ when the $E–R$ excess capacity is exhausted. The capacity model is consistent with unchanged L at an experimental inhibition of E by 50 % [22]. Beyond the first breakpoint, aerobic ATP turnover is compromised ($R⇩$ in phase $E⇩2$). A further decline $E⇩3$ of oxidative capacity then limits leak $L⇩$ below the breakpoint at $\boldsymbol{e*_{E2}} = l°$ at zero coupling efficiency.

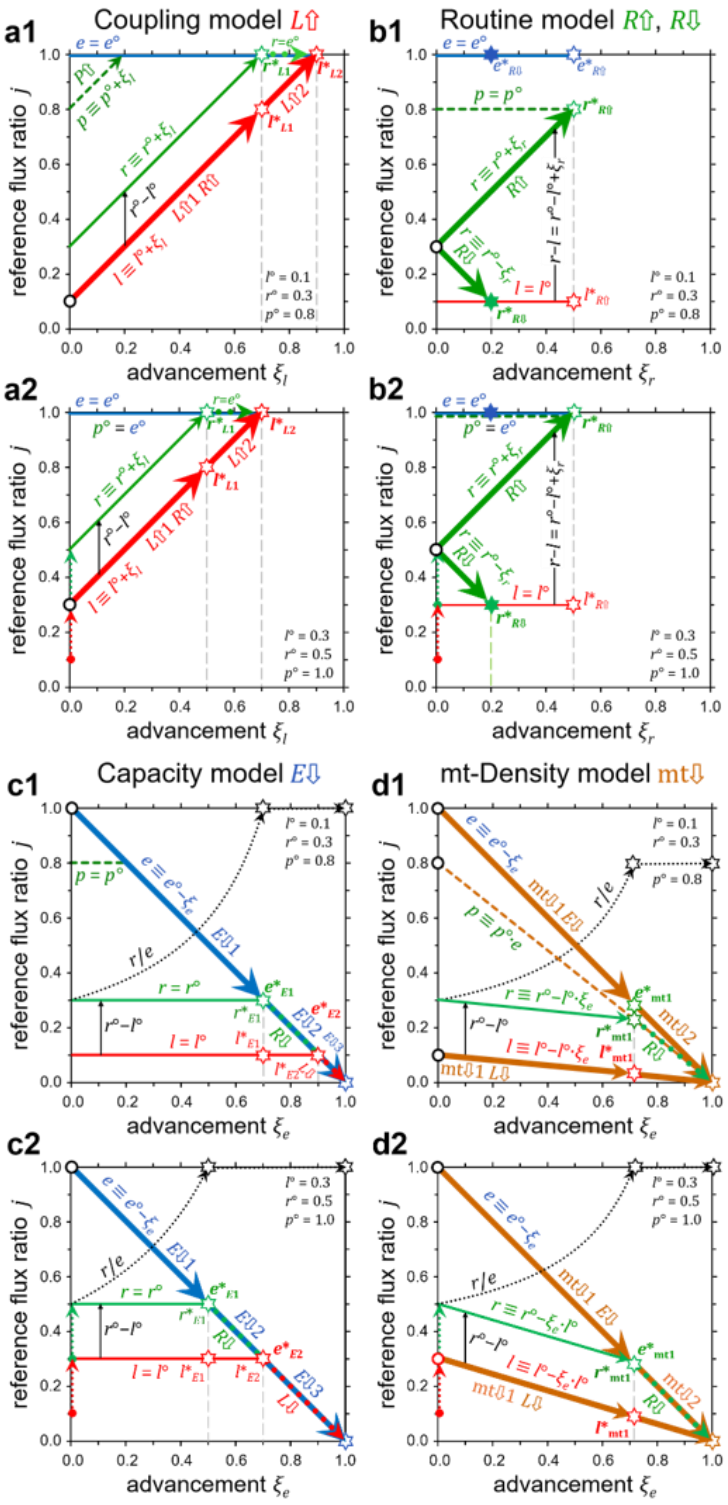

Figure 4. Four models of respiratory control in living cells. Reference flux ratios j are normalized for oxidative capacity $E°$ of the control group. Initial rates are (**1**) $l°$ = 0.1, $r°$ = 0.3, and $p°$ = 0.8, and (**2**) $l°$ = 0.3, $r°$ = 0.5, and $p°$ = 1.0. The controlling flux determines the extent of change in respiratory flux (advancement ξ_j), indicated as thick lines from the control state (circles) to the breakpoints (asterisks) up to which other respiratory parameters are either kept constant or change stoichiometrically to maintain respiratory control efficiencies constant. Beyond the breakpoints, further advancement is not possible without adjustment of other respiratory parameters. **(a) Coupling model** ($L⇧$): progressive increase in L at constant E with compensatory increase $R⇧$ maintaining $r–l$ (and thus ATP turnover) constant up to the breakpoint $\boldsymbol{r^*_{L1}} = e°$. **(b) Routine model** ($R⇧$ or $R⇩$): cell physiological control of aerobic ATP demand increases or decreases routine respiration within the limits of mitochondrial OXPHOS capacity $p°$ and leak respiration $l°$. **(c) Capacity model** ($E⇩$): advancement driven by the decline in e at constant l maintaining $r–l$ (and thus ATP turnover) constant up to the breakpoint $\boldsymbol{e^*_{E1}} = r°$. **(d) mt-Density model** ($mt⇩$): mitochondrial density in the cell declines at constant aerobic ATP turnover (constant $r–l$) up to the breakpoint when $\boldsymbol{r^*_{mt1}/e^*_{mt1}} = p°$, with the corresponding breakpoint $\boldsymbol{e^*_{mt1}} = (r°–l°)/(p°–l°) = j°_{RLE}/j°_{PLE}$ (**Table 1**).

d) mt-Density model (**Figure 4d**): A decline in mitochondrial density in cells is caused by an imbalance of mt-biosynthesis and degradation. If mitochondrial quantity but not quality is affected, then the decline $E\Downarrow$ and $L\Downarrow$ are proportional at a constant L/E ratio and coupling efficiency. In a first phase ($\mathrm{mt}\Downarrow 1$), $R\Downarrow 1$ declines parallel to $L\Downarrow$ at constant ATP-coupled respiration $R{-}L$ to the breakpoint $\boldsymbol{r}^*_{\mathbf{mt1}} = p^\circ\cdot(r^\circ - l^\circ)/(p^\circ - l^\circ) = p^\circ\cdot j^\circ_{RLE}/j^\circ_{PLE}$ while $\boldsymbol{e}^*_{\mathbf{mt1}} = j^\circ_{RLE}/j^\circ_{PLE}$ (**Table 1**). This is followed by further depletion of mt-density in phase $\mathrm{mt}\Downarrow 2$ ($R\Downarrow 2$) at zero $E{-}R$ excess capacity ($r = p$) while the L/E ratio and hence j°_{E-L} are maintained to the breakpoint $\boldsymbol{l}^*_{\mathbf{mt2}} = l^\circ\cdot\boldsymbol{e}^*_{\mathbf{mt2}} = 0$. It is interesting to note that a lower mt-density effectively increases the economy of routine respiration at the expense of the scope of maximal ATP production. The mt-density model thus has direct implications for explaining the apparent hypoxia paradox of unremarkable maximum aerobic capacity at high bioenergetic economy in Tibetan and Sherpa highlanders versus lowlanders [23,24] (see also ref. [25]).

4.2. Relationships of models of flux control

Regression analysis of respiratory control indices versus coupling efficiency show different complementary patterns in response to increasing $L\Uparrow$ or decreasing $E\Downarrow$. Modelling specific mechanisms of respiratory dysfunction provides the background for differential bioenergetic cluster analysis and enhances diagnostic resolution. Respirometric control indices refer to a reference population for diagnostic evaluation.

Changes of respiratory reference flux ratios j with progressive advancement yield the definitions of the breakpoints e^*, l^*, and r^* (**Table 1**). These values can be inserted into the definitions of respiratory control efficiencies (**Box 2**). It is important, therefore, to explicitly introduce e° into these definitions, which otherwise might be dropped (with numerical value 1) for simplification. The breakpoints of respiratory control efficiencies can then be calculated from **Eq. 1**,

$$j^*_{Z-Y} = \frac{Z^* - Y^*}{Z^*} \qquad j^*_{Y_1Y_2Z} = \frac{Y_1^* - Y_2^*}{Z^*} \qquad \text{(Eq. 3)}$$

The solutions of **Eq. 3** yield the breakpoints defined in terms of single initial flux control efficiencies or zero in all models of respiratory control (**Table 2**).

a) $E{-}R$ excess ratio j_{E-R} (**Figure 5a**). When leak respiration increases at constant oxidative capacity, j_{E-R} declines with decreasing coupling efficiency to zero, maintaining $R{-}L$ (reflecting aerobic ATP turnover) constant due to the compensatory increase of R ($L\Uparrow 1$). Beyond $\boldsymbol{R}^*_{\boldsymbol{L1}} = E^\circ$ at the breakpoint $j^*_{E-L(L1)} = j^\circ_{RLE}$, aerobic ATP turnover declines with $L\Uparrow 2$. With decreasing E at constant L ($E\Downarrow 1$), the $E{-}R$ excess ratio declines more steeply with decreasing coupling efficiency at constant R to the breakpoint $j^*_{E-L(E1)} = j^\circ_{R-L}$ ($\boldsymbol{E}^*_{\boldsymbol{E1}} = R^\circ$). Routine respiration declines with further reduction of E ($E\Downarrow 2$). The $E{-}R$ excess ratio can be increased to the maximum value j°_{E-L} by decreasing $R\Downarrow$. j_{E-R} decreases to j°_{E-P} by increasing $R\Uparrow$ or decreasing mt-density $\mathrm{mt}\Downarrow$. The drop of the $R{-}L$ excess ratio with advancement of declining E is shifted to the right in the mt-density model $\mathrm{mt}\Downarrow$ compared to the capacity model $E\Downarrow$.

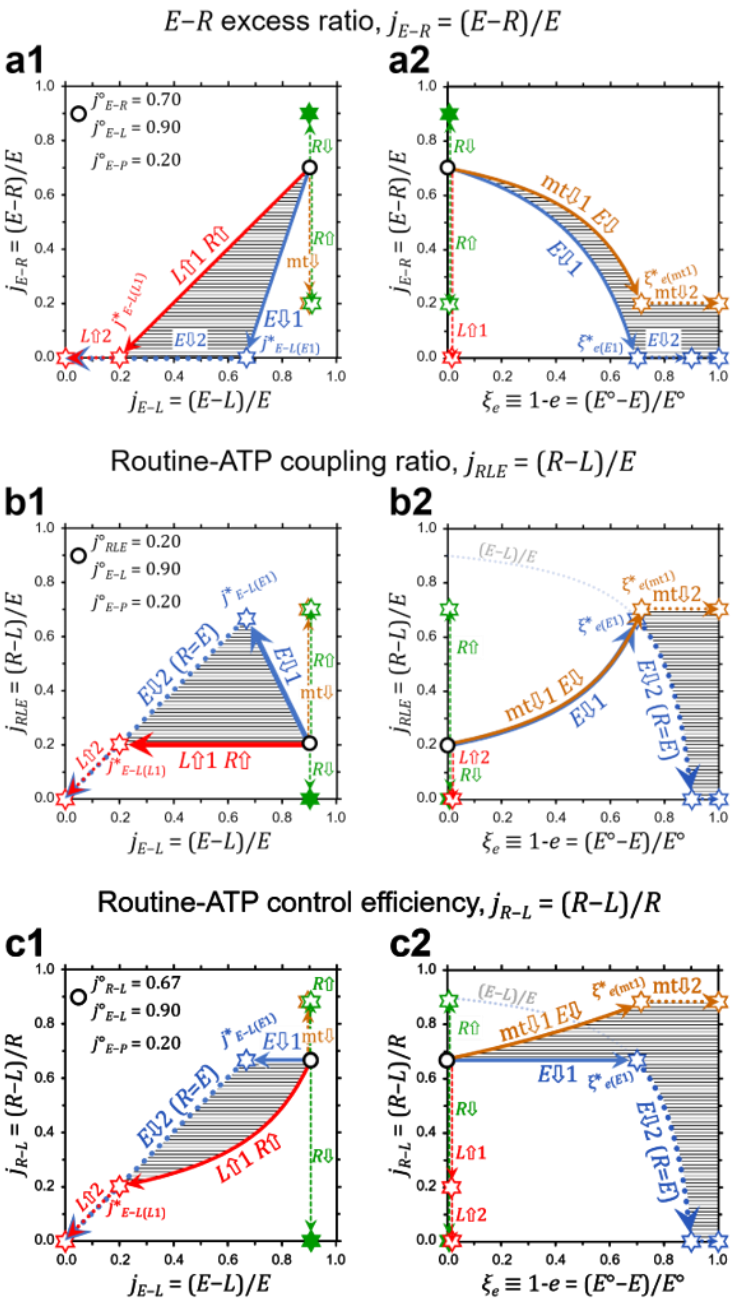

Figure 5. Respiratory control indices as a function of (1) coupling efficiency and (2) advancement of declining ET capacity. Trajectories (arrows) to breakpoints (asterisks) from control or initial states (circles): $l^\circ \stackrel{\text{def}}{=} L^\circ/E^\circ = 0.10$; $r^\circ \stackrel{\text{def}}{=} R^\circ/E^\circ = 0.30$; $p^\circ \stackrel{\text{def}}{=} P^\circ/E^\circ = 0.80$. The vertical axes display **(a)** $E{-}R$ excess ratio, $j^\circ_{E-R} = 0.70$; **(b)** R-ATP coupling ratio, $j^\circ_{RLE} = 0.20$; **(c)** R-ATP control efficiency, $j^\circ_{R-L} = 0.67$. **(1)** Initial coupling efficiency $j^\circ_{E-L} = 0.90$. Red arrows: coupling model ($L\Uparrow$) with breakpoint $j^*_{E-L(L1)} = j^\circ_{RLE}$ ($\boldsymbol{r^*_{L1}} = e^\circ$; $\boldsymbol{l^*_{L1}} = j^\circ_{E-R}{+}l^\circ = 0.80$). Blue arrows: capacity model ($E\Downarrow$); $j^*_{E-L(E1)} = j^\circ_{R-L} = 0.67$ ($\boldsymbol{e^*_{E1}} = r^\circ$). Shaded areas indicate the data space between the coupling and capacity models. Green arrows: routine model ($R\Uparrow$ and $R\Downarrow$), increase and decline of R, respectively, at constant L and E ($\boldsymbol{r^*_{R\Uparrow}} = p^\circ$; and $\boldsymbol{r^*_{R\Downarrow}} = l^\circ$). Brown arrows: mt-density model ($\text{mt}\Downarrow 1$). **(2)** Advancement ξ_e with breakpoints $\xi^*_{e(E1)} = j^\circ_{E-R} = 0.70$ ($E\Downarrow 1$) and $\xi^*_{e(\text{mt}1)} = j^\circ_{PRE}/j^\circ_{PLE} = 0.714$ ($\text{mt}\Downarrow 1$). Shaded areas indicate the data space between the capacity and mt-density models.

b) R-ATP coupling ratio j_{RLE} (**Figure 5b**). When dyscoupling increases leak respiration at constant oxidative capacity E, the compensatory increase of R maintains $R{-}L$ and j_{RLE} constant ($L\Uparrow 1$). The correspondingly increasing R/E° reference flux ratio reaches 1.0 at the breakpoint $j^*_{E-L(L1)} = j^\circ_{RLE}$ (**Table 2**). With further uncoupling ($L\Uparrow 2$), a compensatory increase of R is not possible and j_{RLE} declines with j_{E-L} to zero. However, when E decreases at constant L ($E\Downarrow 1$), j_{RLE} increases linearly with decreasing coupling efficiency, as long as routine respiration remains constant at

$R°$. Beyond the breakpoint ($j^*_{RLE(E1)} = j°_{R-L}$; $\boldsymbol{E^*_{E1}} = R°$), R declines with a further decrease of $E⇩2$ causing a directly proportional drop of j_{RLE} and j_{E-L} to zero. The R-ATP coupling ratio can be increased to the maximum value $j°_{PLE}$ (0.70 in **Figure 5b**) by increasing $R⇧$ or decreasing mt-density mt⇩. The capacity model and mt-density model yield identical trajectories with advancement of declining E to the first breakpoint (**Figure 5b2**).

c) *R*-ATP control efficiency j_{R-L} (**Figure 5c**). With increasing leak respiration $L⇧1$ at constant oxidative capacity E, j_{R-L} declines nonlinearly with decreasing coupling efficiency to the breakpoint $j^*_{R-L(L1)} = j°_{RLE}$ (**Table 2**). On the other hand, j_{R-L} is constant at decreasing E and constant L, as long as R remains constant at $R°$ ($E⇩1$). Beyond the breakpoints $j^*_{E-L(E1)} = j°_{RLE}$ and $\xi^*_{e(E1)} = j°_{E-R}$ (**Table 1**), R declines as $R = E$ with a further decrease of $E⇩2$ causing a directly proportional change of j_{R-L} and j_{E-L} to zero (dotted blue line).

Table 2. Breakpoints of respiratory flux control efficiencies, j^*_1 and j^*_2, in models of respiratory flux control (**Figure 5.1**): coupling ($L⇧$), routine ($R⇧$ and $R⇩$), capacity ($E⇩$), and mt-density (mt⇩) model. Breakpoints are identical for $R⇧$ and mt⇩. For $L⇧$, breakpoints j^*_{E-L}, j^*_{RLE}, and j^*_{R-L} are identical. Similarly for $E⇩$, breakpoints j^*_{E-L}, j^*_{RLE}, and j^*_{R-L} are identical. All breakpoints $L⇧2$ and $E⇩2$ are zero.

	j^*_{E-L}		j^*_{E-R}		j^*_{RLE}		j^*_{R-L}	
$j^*_{L⇧1}$	$j^*_{E-L(L1)}$	$= j°_{RLE}$	$j^*_{E-R(L1)}$	$= 0$	$j^*_{RLE(L1)}$	$= j°_{RLE}$	$j^*_{R-L(L1)}$	$= j°_{RLE}$
$j^*_{L⇧2}$	$j^*_{E-L(L2)}$	$= 0$	$j^*_{E-R(L2)}$	$= 0$	$j^*_{RLE(L2)}$	$= 0$	$j^*_{R-L(L2)}$	$= 0$
$j^*_{R⇧}$	$j^*_{E-L(R⇧)}$	$= j°_{E-L}$	$j^*_{E-R(R⇧)}$	$= j°_{E-P}$	$j^*_{RLE(R⇧)}$	$= j°_{PLE}$	$j^*_{R-L(R⇧)}$	$= j°_{P-L}$
$j^*_{R⇩}$	$j^*_{E-L(R⇩)}$	$= j°_{E-L}$	$j^*_{E-R(R⇩)}$	$= j°_{E-L}$	$j^*_{RLE(R⇩)}$	$= 0$	$j^*_{R-L(R⇩)}$	$= 0$
$j^*_{E⇩1}$	$j^*_{E-L(E1)}$	$= j°_{R-L}$	$j^*_{E-R(E1)}$	$= 0$	$j^*_{RLE(E1)}$	$= j°_{R-L}$	$j^*_{R-L(E1)}$	$= j°_{R-L}$
$j^*_{E⇩2}$	$j^*_{E-L(E2)}$	$= 0$	$j^*_{E-R(E2)}$	$= 0$	$j^*_{RLE(E2)}$	$= 0$	$j^*_{R-L(E2)}$	$= 0$
$j^*_{mt⇩1}$	$j^*_{E-L(mt1)}$	$= j°_{E-L}$	$j^*_{E-R(mt1)}$	$= j°_{E-P}$	$j^*_{RLE(mt1)}$	$= j°_{PLE}$	$j^*_{R-L(mt1)}$	$= j°_{P-L}$
$j^*_{mt⇩2}$	$j^*_{E-L(mt2)}$	$= j°_{E-L}$	$j^*_{E-R(mt2)}$	$= j°_{E-P}$	$j^*_{RLE(mt2)}$	$= j°_{PLE}$	$j^*_{R-L(mt2)}$	$= j°_{P-L}$

4.3. Bioenergetic cluster analysis of young and senescent fibroblasts

Cultured proliferating young and senescent fibroblasts differ in cell size and mitochondrial performance, complicating comparison of cell respiration (**Table 3**). BCA enables distinguishing between the effects of cell size or mitochondrial content per cell and intrinsic mitochondrial performance [6,8].

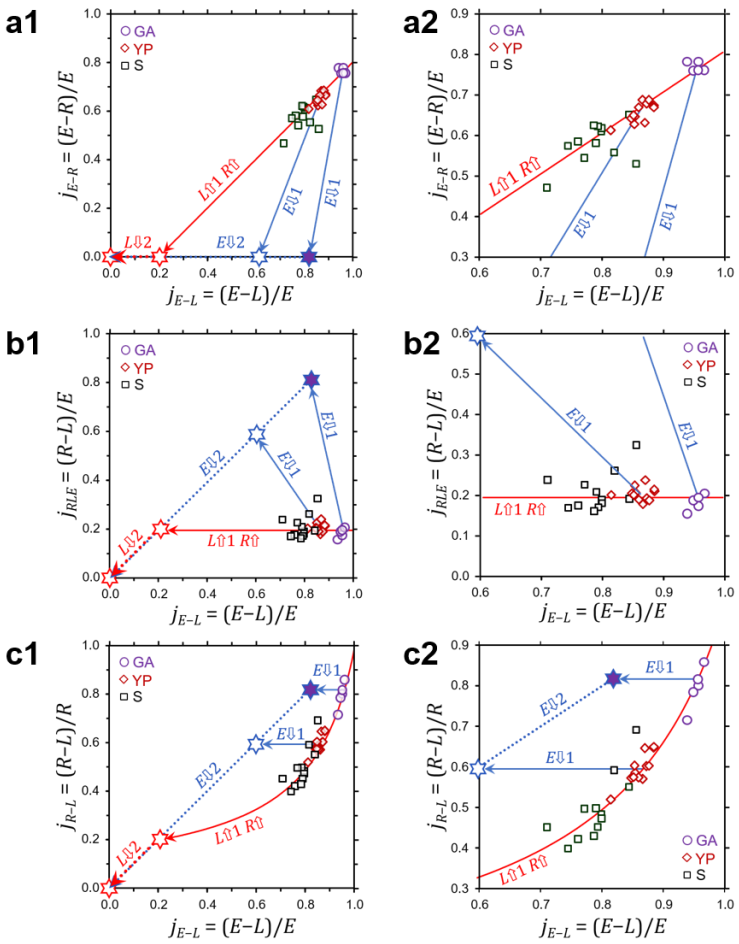

Figure 6. Bioenergetic cluster analysis of respiratory control in growth arrested young (GA), young proliferating (YP), and senescent (S) human foreskin fibroblasts, comparing the coupling and capacity models. Median respiratory control indices of GA and YP cells are shown as reference (**Table 3**). Clusters are isolinear with the $L⇧1$ trajectories, maintaining a large distance to the breakpoints at $R = E°$ (red asterisks). The $L⇧$ trajectories practically overlap (shown for GA only), because $j°_{RLE}$ is nearly identical in GA and YP. Blue full lines are trajectories of changing E at constant L, reaching the breakpoint at $E = R°$ shown for GA (full asterisks) and YP (open blue asterisks). **(1)** Theoretical ranges from 0 to 1. **(2)** Zoom into the experimental data range. **(a)** $E{-}R$ excess ratio diminished in YP and S as a function of R increasing with $L⇧$ and decreasing coupling efficiency. **(b)** j_{RLE} is maintained constant despite varying coupling efficiencies due to changes of L, because R is adjusted accordingly. **(c)** The R-ATP control efficiency changes as a function of varying L.

Table 3. Respiratory attributes of human foreskin fibroblasts (HFF). Young growth arrested cells (GA), young proliferating cells (YP), and senescent cells (S). Original data of routine and leak respiration (R, L), and ET capacity (E) expressed as O_2 flow per cell [amol·s^{-1}·x^{-1}], corrected for residual oxygen consumption rox [amol·s^{-1}·x^{-1}] which is 7.2 (GA), 8.3 (YP), and 17.9 (S), from Hütter et al (2004) [1]. BFI is the bioenergetic fitness index. Values are given as medians; N = 5 (GA) and N = 12 (YP and S).

HFF	R	L	E	$(E{-}L)/E$	$(R{-}L)/E$	$(R{-}L)/R$	$(E{-}R)/E$	BFI
	amol·s^{-1}·x^{-1}	amol·s^{-1}·x^{-1}	amol·s^{-1}·x^{-1}	j_{E-L}	j_{RLE}	j_{R-L}	j_{E-R}	j_{RLE}·j_{E-L}·100
GA	32.5	5.9	135.8	0.96	0.19	0.80	0.76	17.9
YP	39.2	14.8	108.8	0.86	0.20	0.59	0.66	17.2
S	120.5	59.4	287.4	0.79	0.19	0.48	0.58	15.6

The bioenergetic clusters of senescent (S) and young proliferating (YP) human foreskin fibroblasts [1] are isolinear with the trajectories of changing L at constant group-specific E° (but E° differs between groups, doubling in S; **Table 3**). This points to an increase of leak respiration causing dyscoupling in senescent cells in line with the coupling model (**Figure 6**). Nevertheless, the bioenergetic fitness index (**Section 5**) is largely maintained in S due to the constant routine-ATP coupling ratio j_{RLE}.

5. Bioenergetic fitness index BFI

The bioenergetic health index (BHI) is a mathematical framework for condensing the bioenergetic profile of living cells into a single value [26]. Despite its formal appeal, the BHI had limited influence on the scientific community, generating neither widespread adoption nor substantial critical discussion in the peer-reviewed literature. In contrast, it gained popularity in the biohacking community. A critical analysis of the BHI motivated the development of the BFI, combining the coupling-control indices of living cells in a single composite score. It remains questionable, if the BFI as a single composite index is helpful or – like any single index – inadequate to capture the complexities of mitochondrial function and dysfunction (**Table 3**).

Efficiencies range from 0 to 1 (0 to 100 %). Similarly, the BFI ranges theoretically from 0 to 100 (https://wiki.oroboros.at/index.php/Bioenergetic_fitness_index_BFI, retrieved 2026-09-21). The $E{-}R$ excess ratio is high in many cell types and the corresponding R-ATP coupling ratio is less than 0.3. Then the BFI is practically restricted by cell physiological rather than mitochondrial control at $j_{RLE} < 0.3$ to a range <30:

$$\mathrm{BFI} = j_{RLE} \cdot j_{E\text{–}L} \cdot 100 = (R{-}L)/E \cdot (E{-}L)/E \cdot 100 \qquad \text{(Eq. 4)}$$

Like any respiratory ratio, the BFI reduces respirometric information to the numerical aspect of mitochondrial quality. A core concept of the BFI is the normalization of differences of respiratory activities in different coupling states by the electron transfer capacity E as the reference state. The physiologically relevant parameter of mitochondrial content or concentration in a cell or tissue is not expressed by the BFI and respiratory control efficiencies. Thus, the BFI must be contextualized in a cascade of quantitative relationships, from mitochondrial bioenergetic quality (BFI, j_{RLE}, coupling efficiency, etc.), to respiratory capacity per cell (E, R, L), to mitochondrial density in a cell, cell size, cell concentration, cell count (or mass or volume) in a tissue, to the tissue size and tissue composition of the whole organism.

6. Discussion

Several hundred publications report results on cell respiration obtained with the basic coupling control protocol (CCP). The term ‘stress’ remains ambiguous when ‘Cell Mito Stress Test’ is applied as a brand name for this assay [5], comparable to the

widely used term oxidative ‘stress’ [27]. Most studies applying the CCP do not provide the detailed analysis and interpretation of respiratory control by bioenergetic cluster analysis. Notably, many peer-reviewed publications report ‘maximal’ ET capacity below routine respiration [5], thus failing a fundamental quality-control criterion based on flux-control ratios: theoretically, $R/E>1$ is impossible. Such artifacts may result from sub- or supra-optimal uncoupler concentrations leading to underestimation of ET-capacity [5,12,28] and from excessively high oligomycin concentrations exerting off-target inhibition of ET-capacity [3,29]. Without adequate conceptual screening by BCA for quality control including outlier detection [7], key tasks in cell bioenergetics remain unresolved.

Respiratory control ratios and control efficiencies provide valuable quantitative information on mt-quality and routine respiratory function of living cells. However, changes in the balance between mt-biogenesis and degradation must be evaluated by expressing results as respiratory capacities (O_2 flow per cell, O_2 flux per cell size, or per tissue mass). Mitochondria are stimulated to proliferate by aerobic endurance training, representing the most successful treatment of numerous degenerative diseases including obesity and diabetes 2. Even against this wide-ranging background, the concept of mitochondrial health remains overcast by uncertainties whether more or less mitochondria is good or bad [30,31,32]. A decrease in mitochondrial density or coupling efficiency may represent physiological adaption to a challenge within a range beyond which it becomes indicative of mitochondrial dysfunction. Trajectories between control states and their breakpoints in BCA provide a unique quantitative framework for defining the scope of metabolic flexibility.

The direction of a bioenergetic change does not necessarily define improvement versus loss of functional mitochondrial fitness, and current interpretations are strongly influenced by experimental context. Consider contrasting interpretations of mild uncoupling and reactive oxygen species as damaging effectors versus signaling events, or of bioenergetic changes associated with exercise and caloric restriction versus T2 diabetes in adipose-mass-matched controls. Such context-dependent uncertainties raise a broader question: Are common interpretations of drug effects similarly biased by preconceived models of mitochondrial fitness? The same direction of bioenergetic interference may encompass therapeutic efficacy at moderate intensity and adverse effects beyond a tipping point: ‘moderate interference should be considered as a basis for therapeutic efficacy’ [33]. Evaluation of such tipping points between physiological adaption and emerging dysfunction moves beyond conventional paradigms of continuous progression toward either injury or improvement. Paralleling broader debates on the distinction between clinical illness and health [34], the unambiguous distinction between mitochondrial dysfunction and mitochondrial health remains a conceptual challenge.

7. Conclusions

In contrast to a merely descriptive presentation of results, BCA provides quality control by identifying apparent experimental artifacts. More importantly, BCA reveals fundamental bioenergetic mechanisms that drive respiratory changes and thereby provides a basis for addressing the major challenge of distinguishing regulatory physiological adaption or evolutionary adaptation from degenerative dysfunction. Evolutionary adaptations provide unique models for differentiating functional adjustments from injury, provided that functionally neutral adaptations can be excluded. Implementation of BCA is an important step toward mapping the scope of metabolic flexibility for improved evaluation of mitochondrial fitness.

Terms and abbreviations

BCA	bioenergetic cluster analysis
BFI	bioenergetic fitness index
BHI	bioenergetic health index
E	oxidative capacity = electron transfer capacity; $E°$ = E in initial state
e	= $E/E°$; oxidative reference flux ratio; $e°$ = $E°/E°$ = 1; $e*$ = e at breakpoint
ET	electron transfer
ETS	electron transfer system
j_{RLE}	routine-ATP coupling ratio, $(R-L)/E$
j_{E-L}	coupling efficiency, oxidative coupling-control efficiency, $(E-L)/E$
j_{E-R}	$E-R$ excess ratio, $(E-R)/E$
j_{R-L}	routine-ATP control efficiency, $(R-L)/R$
L	leak rate of respiration; $l°$ = $L°/E°$ in initial state
l	= $L/E°$; leak reference flux ratio; $l°$ = $L°/E°$; $l*$ = l at breakpoint
L/E	flux control ratio measured in a particular cell population
OXPHOS	oxidative phosphorylation
P	OXPHOS capacity; $p°$ = $P°/E°$ in initial state
p	= $P/E°$; OXPHOS reference flux ratio
R	routine respiration; $R°$ = R in initial state
r	= $R/E°$; routine reference flux ratio; $r°$ = $R°/E°$; $r*$ = r at breakpoint
R/E	flux control ratio measured in the coupling-control protocol
rox	residual oxygen consumption
SUIT	substrate-uncoupler-inhibitor titrations
x	unit of the count of a specified entity, e.g., of the number of cells
ν_j	stoichiometric number of rate j
ξ_j	= $(j-j°)/\nu_j$; advancement of the change in rate j

Acknowledgements

I thank Luiza Cardoso, Natália Huňarová, Elettra Leo, Elisa Mezzadri, Alejandra Romero-Martinez, and Jaime Willis for helpful discussions. This work was supported by the K-Regio enterprise

project MitoDrugs, funded by Standortagentur Tirol and the State of Tyrol, and co-funded by the European Union (EFRE).

References

1. Hütter E, Renner K, Pfister G, Stöckl P, Jansen-Dürr P, Gnaiger E (2004) Senescence-associated changes in respiration and oxidative phosphorylation in primary human fibroblasts. Biochem J 380:919-28. https://doi.org/10.1042/BJ20040095
2. Brand MD, Nicholls DG (2011) Assessing mitochondrial dysfunction in cells. Biochem J 435:297-312. https://doi.org/10.1042/BJ20110162
3. Zdrazilova L, Hansikova H, Gnaiger E (2022) Comparable respiratory activity in attached and suspended human fibroblasts. PLoS ONE 17:e0264496. https://doi.org/10.1371/journal.pone.0264496
4. Gnaiger E (2025) Mitochondrial respiratory function in living cells. Bioenerg Commun 2025.5. https://doi.org/10.26124/bec.2025-0005
5. Ransy C, Boissan M, Hammad N, Bouaboud A, Issad T, De Dieuleveult M, Miotto B, Ye M, Pasmant E, Bouillaud F (2026) Extracellular flux analyses indicate low ATP yield and require refinement for accurate determination of maximal oxygen consumption rate. Sci Rep 16:18344. https://doi.org/10.1038/s41598-026-46479-w
6. Gnaiger E (2020) Mitochondrial pathways and respiratory control. An introduction to OXPHOS analysis. 5th ed. Bioenerg Commun 2020.2. https://doi.org/10.26124/bec:2020-0002
7. Gnaiger E (2021) Bioenergetic cluster analysis – mitochondrial respiratory control in human fibroblasts. MitoFit Preprints 2021.8. https://doi.org/10.26124/mitofit:2021-0008
8. Gnaiger E et al — MitoEAGLE Task Group (2020) Mitochondrial physiology. Bioenerg Commun 2020.1. https://doi.org/10.26124/bec:2020-0001.v1
9. Drahota Z, Milerová M, Stieglerová A, Houstek J, Ostádal B (2004) Developmental changes of cytochrome c oxidase and citrate synthase in rat heart homogenate. Physiol Res 53:119-22.
10. Kamienieva I, Charzyńska A, Duszyński J, Malińska D, Szczepanowska J (2023) In search for mitochondrial biomarkers of Parkinson's disease: findings in parkin-mutant human fibroblasts. Biochim Biophys Acta Mol Basis Dis 1869:166787. https://doi.org/10.1016/j.bbadis.2023.166787
11. Fiorani M, Buffi G, Bagherlou N, Canonico B, De Matteis R, Guidarelli A, Montanari M, Battistelli M, Papa S, Coppo L, Cerioni L, Spina A, Cantoni O (2025) Clozapine blunts mitochondrial biogenesis in differentiating adipocytes: The increased ATP demand is met via stimulation of electron transport chain expression and activity in residual mitochondria. Biochim Biophys Acta Mol Cell Res 1872:119967. https://doi.org/10.1016/j.bbamcr.2025.119967
12. Gnaiger E (2008) Polarographic oxygen sensors, the oxygraph and high-resolution respirometry to assess mitochondrial function. In: Mitochondrial dysfunction in drug-induced toxicity (Dykens JA, Will Y, eds) John Wiley & Sons, Inc, Hoboken, NJ:327-52.
13. Chance B, Williams GR (1955) Respiratory enzymes in oxidative phosphorylation. I. Kinetics of oxygen utilization. J Biol Chem 217:383-93.
14. Timón-Gómez A, Doerrier C, Sumbalová Z, Garcia-Souza LF, Baglivo E, Cardoso LHD, Gnaiger E (2026) Bioenergetic profiles and respiratory control in mitochondrial physiology: Precision analysis of oxidative phosphorylation. Exp Physiol 111:179-211. https://doi.org/10.1113/EP092792

15. Cardoso LHD, Gnaiger E (2024) OXPHOS coupling and uncoupling. Bioenerg Commun 2024.5. https://doi.org/10.26124/bec.2024-0005
16. FAO/WHO/UNU (2004) Human Energy Requirements. Report of a Joint FAO/WHO/UNU Expert Consultation. FAO Food and Nutrition Technical Report Series No. 1. Food and Agriculture Organization, Rome.
17. Reynolds JA, Hand SC (2004) Differences in isolated mitochondria are insufficient to account for respiratory depression during diapause in *Artemia franciscana* embryos. Physiol Biochem Zool 77:366-77. https://doi.org/10.1086/420950
18. Brett CMA, Frey JG, Hinde R, Kuroda Y, Marquardt R, Pavese F, Quack M, Stohner J, Thor AJ (eds) (2023) Quantities, Units and Symbols in Physical Chemistry, 4th ed, Abridged Version. Royal Society of Chemistry. https://doi.org/10.1039/9781839163180
19. Gnaiger E (2025) Protonmotive force - from motive protons to membrane potential. Bioenerg Commun 2025.7. https://doi.org/10.26124/bec.2025-0007
20. Hochachka PW, Somero GN (2002) Biochemical adaptation: mechanism and process in physiological evolution. Oxford Univ Press, New York: 466 pp.
21. Lemieux H, Semsroth S, Antretter H, Höfer D, Gnaiger E (2011) Mitochondrial respiratory control and early defects of oxidative phosphorylation in the failing human heart. Int J Biochem Cell Biol 43:1729–38. https://doi.org/10.1016/j.biocel.2011.08.008
22. Krumschnabel G, Eigentler A, Fasching M, Gnaiger E (2014) Use of safranin for the assessment of mitochondrial membrane potential by high-resolution respirometry and fluorometry. Methods Enzymol 542:163-81. https://doi.org/10.1016/B978-0-12-416618-9.00009-1
23. Marconi C, Marzorati M, Cerretelli P (2006) Work capacity of permanent residents of high altitude. High Alt Med Biol 7:105-15. https://doi.org/10.1089/ham.2006.7.105
24. Horscroft JA, Kotwica AO, Laner V, West JA, Hennis PJ, Levett DZH, Howard DJ, Fernandez BO, Burgess SL, Ament Z, Gilbert-Kawai ET, Vercueil A, Landis BD, Mitchell K, Mythen MG, Branco C, Johnson RS, Feelisch M, Montgomery HE, Griffin JL, Grocott MPW, Gnaiger E, Martin DS, Murray AJ (2017) Metabolic basis to Sherpa altitude adaptation. Proc Natl Acad Sci U S A 114:6382–7. https://doi.org/10.1073/pnas.1700527114
25. Gnaiger E, Boushel R, Søndergaard H, Munch-Andersen T, Damsgaard R, Hagen C, Díez-Sánchez C, Ara I, Wright-Paradis C, Schrauwen P, Hesselink M, Calbet JAL, Christiansen M, Helge JW, Saltin B (2015) Mitochondrial coupling and capacity of oxidative phosphorylation in skeletal muscle of Inuit and caucasians in the arctic winter. Scand J Med Sci Sports 25 (Suppl 4):126–34. https://doi.org/10.1111/sms.12612
26. Chacko BK, Kramer PA, Ravi S, Benavides GA, Mitchell T, Dranka BP, Ferrick D, Singal AK, Ballinger SW, Bailey SM, Hardy RW, Zhang J, Zhi D, Darley-Usmar VM (2014) The bioenergetic health index: A new concept in mitochondrial translational research. Clin Sci (Lond) 127:367-73. https://doi.org/10.1042/CS20140101
27. Azzi A (2022) Oxidative stress: What is it? Can it be measured? Where is it located? Can it be good or bad? Can it be prevented? Can it be cured? Antioxidants (Basel) 11:1431. https://doi.org/10.3390/antiox11081431
28. Steinlechner-Maran R, Eberl T, Kunc M, Margreiter R, Gnaiger E (1996) Oxygen dependence of respiration in coupled and uncoupled endothelial cells. Am J Physiol Cell Physiol 271:C2053-61. https://doi.org/10.1152/ajpcell.1996.271.6.C2053
29. Ruas JS, Siqueira-Santos ES, Amigo I, Rodrigues-Silva E, Kowaltowski AJ, Castilho RF (2016) Underestimation of the maximal capacity of the mitochondrial electron transport

system in oligomycin-treated cells. PLOS ONE 11:e0150967. https://doi.org/10.1371/journal.pone.0150967
30. Freyer C, Larsson NG (2007) Is energy deficiency good in moderation? Cell 131:448-50. https://doi.org/10.1016/j.cell.2007.10.027
31. Pospisilik JA, Knauf C, Joza N, Benit P, Orthofer M, Cani PD, Ebersberger I, Nakashima T, Sarao R, Neely G, Esterbauer H, Kozlov A, Kahn CR, Kroemer G, Rustin P, Burcelin R, Penninger JM (2007) Targeted deletion of aif decreases mitochondrial oxidative phosphorylation and protects from obesity and diabetes. Cell 131:476-91. https://doi.org/10.1016/j.cell.2007.08.047
32. Brunetta HS, de Paula GC, de Oliveira J, Martins EL, Dos Santos GJ, Galina A, Rafacho A, de Bem AF, Nunes EA (2019) Decrement in resting and insulin-stimulated soleus muscle mitochondrial respiration is an early event in diet-induced obesity in mice. Exp Physiol 104:306-321. https://doi.org/10.1113/EP087317
33. Hammad N, Ransy C, Pinson B, Talmasson J, Bréchot C, Rossignol JF, Bouillaud F (2024) Nitazoxanide controls virus viability through its impact on membrane bioenergetics. Sci Rep 14:30679. https://doi.org/10.1038/s41598-024-78694-8
34. Rubino F, Cummings DE, Eckel RH, Cohen RV, Wilding JPH, Brown WA, Stanford FC, Batterham RL, Farooqi IS, Farpour-Lambert NJ, le Roux CW, Sattar N, Baur LA, Morrison KM, Misra A, Kadowaki T, Tham KW, Sumithran P, Garvey WT, Kirwan JP, Fernández-Real JM, Corkey BE, Toplak H, Kokkinos A, Kushner RF, Branca F, Valabhji J, Blüher M, Bornstein SR, Grill HJ, Ravussin E, Gregg E, Al Busaidi NB, Alfaris NF, Al Ozairi E, Carlsson LMS, Clément K, Després JP, Dixon JB, Galea G, Kaplan LM, Laferrère B, Laville M, Lim S, Luna Fuentes JR, Mooney VM, Nadglowski J Jr, Urudinachi A, Olszanecka-Glinianowicz M, Pan A, Pattou F, Schauer PR, Tschöp MH, van der Merwe MT, Vettor R, Mingrone G (2025) Definition and diagnostic criteria of clinical obesity. Lancet Diabetes Endocrinol 13:221-62. https://doi.org/10.1016/S2213-8587(24)00316-4.